Current Biology 19, 253–259, February 10, 2009 ©2009 Elsevier Ltd All rights reserved DOI 10.1016/j.cub.2008.12.044

Report

Neutrophils Establish Rapid and Robust WAVE Complex Polarity in an Actin-Dependent Fashion

Arthur Millius,[1,2] Sheel N. Dandekar,[1,2] Andrew R. Houk,[1,2] and Orion D. Weiner[1,*]

[1]Cardiovascular Research Institute and Department of Biochemistry
600 16th Street, Genentech Hall, S474
University of California, San Francisco
San Francisco, CA 94158
USA

Summary

Asymmetric intracellular signals enable cells to migrate in response to external cues. The multiprotein WAVE (also known as SCAR or WASF) complex activates the actin-nucleating Arp2/3 complex [1–4] and localizes to propagating "waves," which direct actin assembly during neutrophil migration [5, 6]. Here, we observe similar WAVE complex dynamics in other mammalian cells and analyze WAVE complex dynamics during establishment of neutrophil polarity. Earlier models proposed that spatially biased generation [7] or selection of protrusions [8] enables chemotaxis. These models require existing morphological polarity to control protrusions. We show that spatially biased generation and selection of WAVE complex recruitment also occur in morphologically unpolarized neutrophils during development of their first protrusions. Additionally, several mechanisms limit WAVE complex recruitment during polarization and movement: Intrinsic cues restrict WAVE complex distribution during establishment of polarity, and asymmetric intracellular signals constrain it in morphologically polarized cells. External gradients can overcome both intrinsic biases and control WAVE complex localization. After latrunculin-mediated inhibition of actin polymerization, addition and removal of agonist gradients globally recruits and releases the WAVE complex from the membrane. Under these conditions, the WAVE complex no longer polarizes, despite the presence of strong external gradients. Thus, actin polymer and the WAVE complex reciprocally interact during polarization.

Results and Discussion

For neutrophils, the WAVE complex is required for motility and polarity, exhibits propagating waves generated through rapid sequential rounds of recruitment and release of the complex from the plasma membrane, and requires actin polymer for its recycling from the plasma membrane [6]. Several pieces of evidence suggest that similar WAVE complex dynamics organize protrusion in other metazoan cells: The WAVE complex is required for the movement and morphogenesis of cells in *C. elegans* [9], *Drosophila* [10, 11], and mice [3, 12]; the WAVE complex localizes to the tips of protruding lamellipodia in B16F10 murine melanoma cells [13] (Figure 1A and Movie S1 available online); and this leading-edge localization represents rapidly cycling WAVE complex (a half-life of 8.6 s for WAVE in murine melanoma cells compared to 6.4 s for the Hem-1 component of the neutrophil WAVE complex [6, 14]). To determine whether actin assembly is required for WAVE complex recycling in cells other than neutrophils, we depolymerized the actin cytoskeleton in B16F10 cells expressing a fluorescently tagged subunit of the WAVE complex (Abi1). Actin disassembly resulted in cessation of WAVE complex movement and significant WAVE complex enrichment (2.4 ± 0.3 fold, $p < .005$) near the plasma membrane (Figure 1B and Movie S2), suggesting that actin is also required for WAVE complex recycling in these cells. Collectively, these data suggest that the WAVE complex exhibits similar properties in diverse mammalian cells and is probably a general regulator of cell migration throughout metazoans.

WAVE complex dynamics exhibit several features that make them ideal for a quantitative readout of polarity in neutrophils as compared to other internal signals such as the phospholipid PIP_3 [15–17] or cell morphology [7, 8, 18]. PIP_3 now appears to be dispensable for chemotaxis in neutrophils [19] and *Dictyostelium* [20]. Morphology results from the integration of many signals. Compared to previous morphological studies [7, 8], our use of total internal reflection fluorescence (TIRF) imaging only visualizes the footprint of the cell and is likely to emphasize stabilized protrusions versus protrusions that are unlinked to the surface.

To compare WAVE complex dynamics and cell morphology as readouts for polarity, we analyzed cells after exposure to chemoattractant gradients (Figures 1C and 1D and Movie S3). We developed automated image-analysis software (Figure S1) to quantify the relation between agonist perturbations and WAVE complex response for a large number of cells. When a micropipette containing agonist was moved to a new location, WAVE complex recruitment changed more dramatically in the following 10 s than did cell morphology (Figure 1C, compare 84 s to 94 s). For quiescent cells exposed to gradients of chemoattractant, significant WAVE complex asymmetry was observed in the absence of obvious morphological polarity (Figure 2B, 14 s time point). We examined these cells to determine how morphological protrusions and WAVE complex behavior relate to the external gradient. Both were highly accurate in predicting the ultimate gradient direction. However, protrusions oscillated significantly around the true gradient direction (SD = 24%), whereas changes in WAVE complex behavior were more precisely aligned with the gradient (SD = 12%). These data suggest that under our stimulation conditions, changes in WAVE complex dynamics represent a more quantitative and robust readout of polarity than does cell morphology.

The establishment of WAVE complex asymmetry was determined by analyzing the signaling response of an initially quiescent cell to chemoattractant (Figure 2A). Quiescent cells were exposed to a range of agonist increases and split into two equal-size populations on the basis of the size of the mean estimated increase in fractional receptor occupancy (see Supplemental Experimental Procedures; 0.63 was the median increase). Among our micropipette experiments, the average

*Correspondence: orion.weiner@ucsf.edu
[2]These authors contributed equally to this work.

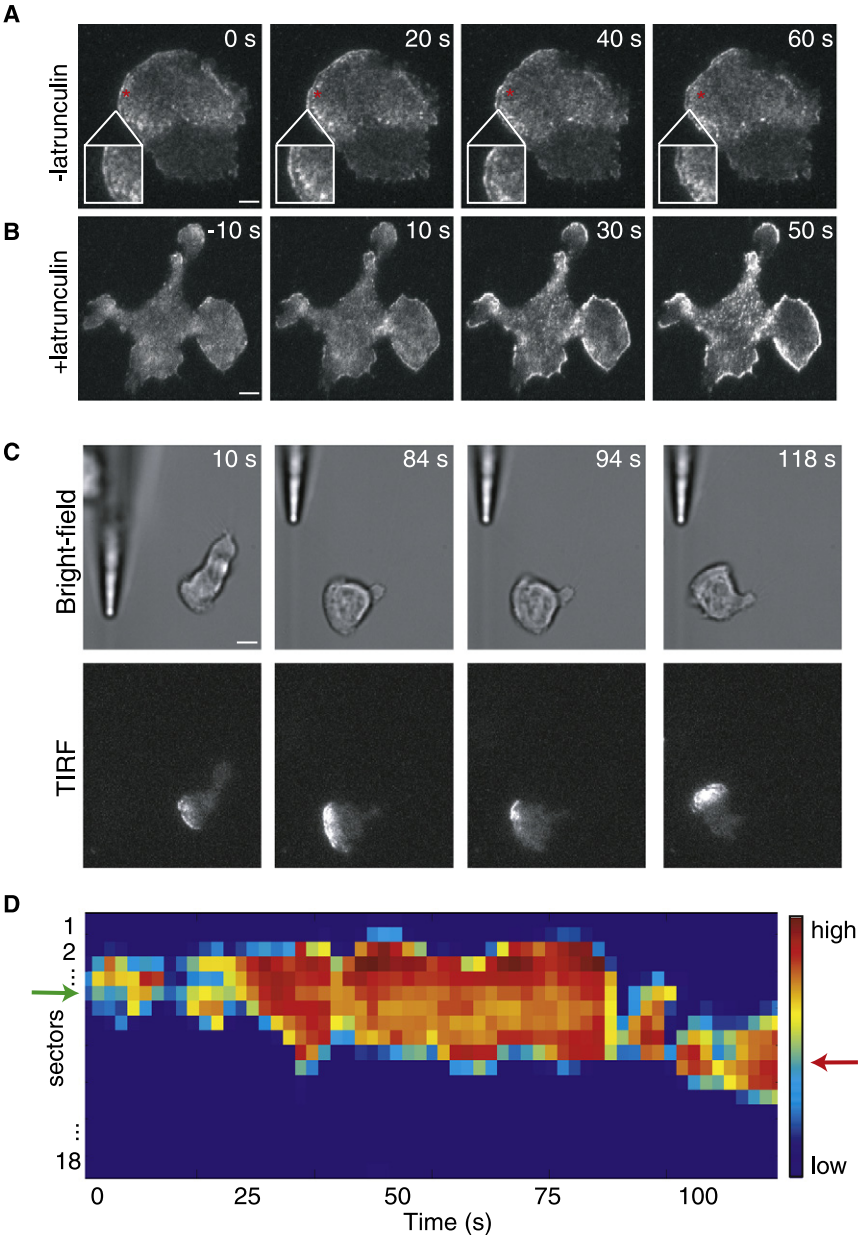

Figure 1. Propagating Waves of the WAVE Complex Are Mechanistically Conserved in Other Mammalian Cells and Represent a Dynamic Quantitative Polarity Readout in Neutrophils

(A) Representative TIRF time-lapse sequences for a B16F10 fibroblast cell migrating on fibronectin expressing Abi1 (a component of the WAVE complex) tagged with YFP. As in HL-60 cells, propagating waves of the WAVE complex are observed at the leading edge (Movie S1). The red asterisk represents a stationary fiduciary mark indicating WAVE complex movement.

(B) Representative Abi1-YFP TIRF time-lapse sequences for a migrating B16F10 fibroblast exposed to 10 μM latrunculin at 0 s. Similar to HL-60 cells, B16F10 cells exhibit an enrichment of WAVE complex near the membrane after latrunculin treatment, suggesting a role for actin polymer in WAVE complex recycling (Movie S2).

(C) Representative bright-field and Hem1-YFP TIRF time-lapse sequences for a HL-60 cell executing a turn in response to a change in the direction of the agonist gradient (Movie S3).

(D) Corresponding heat map shows wave response. The green arrow indicates the initial up-gradient direction; the red arrow indicates the final up-gradient direction. Bars represent 5 μm.

receptor-occupancy change correlated better with cell response than did the slope of the gradient (data not shown). Cells exposed to increases in estimated mean receptor occupancy from 0 to < 0.63 responded to the new gradient with focused generation of WAVE complex recruitment (Figures 2B and 2D and Movie S4). For mean receptor-occupancy increases greater than 0.63, most cells produced a relatively uniform distribution of WAVE complex recruitment that collapsed into a focused distribution on the up-gradient surface (Figures 2C and 2D and Movie S5). In both cases, WAVE complex asymmetry ultimately aligns with the external agonist gradient.

Previous analyses of uniformly stimulated neutrophils showed initially uniform signaling responses before cells became polarized [6, 17]. It is unknown whether cells can also produce initially asymmetric signaling in response to uniform stimulation. To test this possibility, we observed the responses of quiescent cells (when cells lost all WAVE complex dynamics and any obvious morphological front and back). A mean receptor-occupancy increase from 0 to 0.1 caused the cells to produce focused WAVE complex recruitment (Figures 3A and 3C and Movie S6). In contrast, a mean receptor-occupancy increase from 0 to 0.7 caused cells to produce a spatially uniform distribution of WAVE complex recruitment that ultimately collapsed into a focused distribution (Figures 3B and 3C and Movie S7). The first detectable response in either case occurred approximately 12–18 s after stimulation. These data suggest that immediate signaling asymmetries are generated in response to small agonist steps. Previous studies examining the establishment of PIP_3 asymmetry [17] and WAVE asymmetry [6] used larger increases in receptor occupancy, conditions that prevent the initially focused recruitment of WAVE complex in response to uniform chemoattractant (Figures 3B and 3C).

There are several potential mechanisms that could constrain WAVE complex dynamics to a limited region of the cell surface. For instance, upstream molecular asymmetries could act to restrict WAVE complex recruitment to a limited region of the cell surface during the establishment of polarity. An example of this type of internal directional bias is centrosome position, which influences the initial axis of morphological polarity in response to uniform chemoattractant [21]. This sort of intrinsic bias could be responsible for the immediate WAVE complex polarity in response to small steps in uniform chemoattractant (Figure 3A). A second source of internal directional bias could operate during migration. Moving cells have polarized morphologies and intracellular signals, which act as a directional bias to restrict protrusions near the existing leading edge [18, 22]. This type of internal directional bias spatially

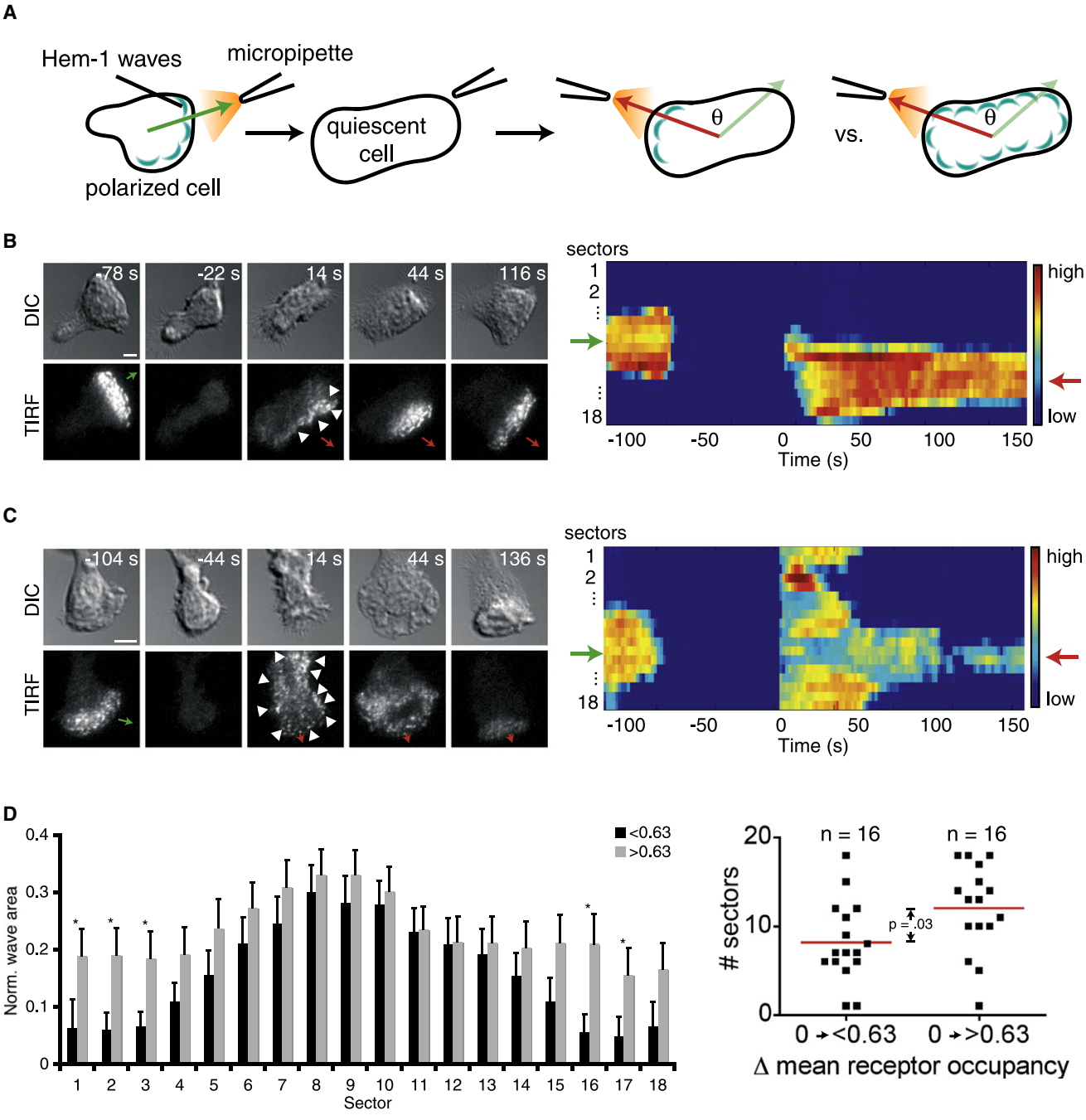

Figure 2. Cells Establish Hem-1 Wave Asymmetry through Either Focused Generation or Uniform Generation Followed by Selection

(A) Illustration of experimental setup. An agonist gradient was applied to a cell and then removed. This process was necessary to ensure quiescence because cells adhered to a coverslip often exhibited polarity and motility even in the absence of chemoattractant. Cells were classified as quiescent when they lost all wave dynamics and any obvious morphological front and back. The micropipette was repositioned at a different angle and the gradient was reapplied at t = 0 s. Therefore, all cells start with a mean receptor occupancy of 0 for this figure. The angle difference and interval between agonist applications did not affect WAVE complex distribution, nor did the cell retain memory of the original micropipette position after the micropipette was turned back on (Figure S2).

(B and C) Representative differential interference contrast (DIC) and Hem-1-YFP TIRF time-lapse sequences and corresponding heat maps show that cells exhibit a focused (B) (Movie S4) or uniform (C) (Movie S5) distribution of waves. Note that wave asymmetry is apparent in the absence of any obvious morphological differences (as indicated by arrowheads). Green arrows indicate initial the up-gradient direction; red arrows indicate the final up-gradient direction. Bars represent 5 μm.

(D) Bar graph (left) of a 20 s average of wave response immediately after gradient reapplication. Black bars show response for cells with mean receptor occupancy (poststimulation) of < 0.63. Gray bars indicate cells with mean receptor occupancy (poststimulation) of >0.63. Error bars represent the standard error of the mean (SEM). Asterisks indicate statistically significant differences between means of each sector ($p < 0.05$, Student's t test). The dot plot (right) shows a statistically significant difference ($p = .03$, Student's t test) between the mean widths (red lines) of the distributions as defined in Figure S1.

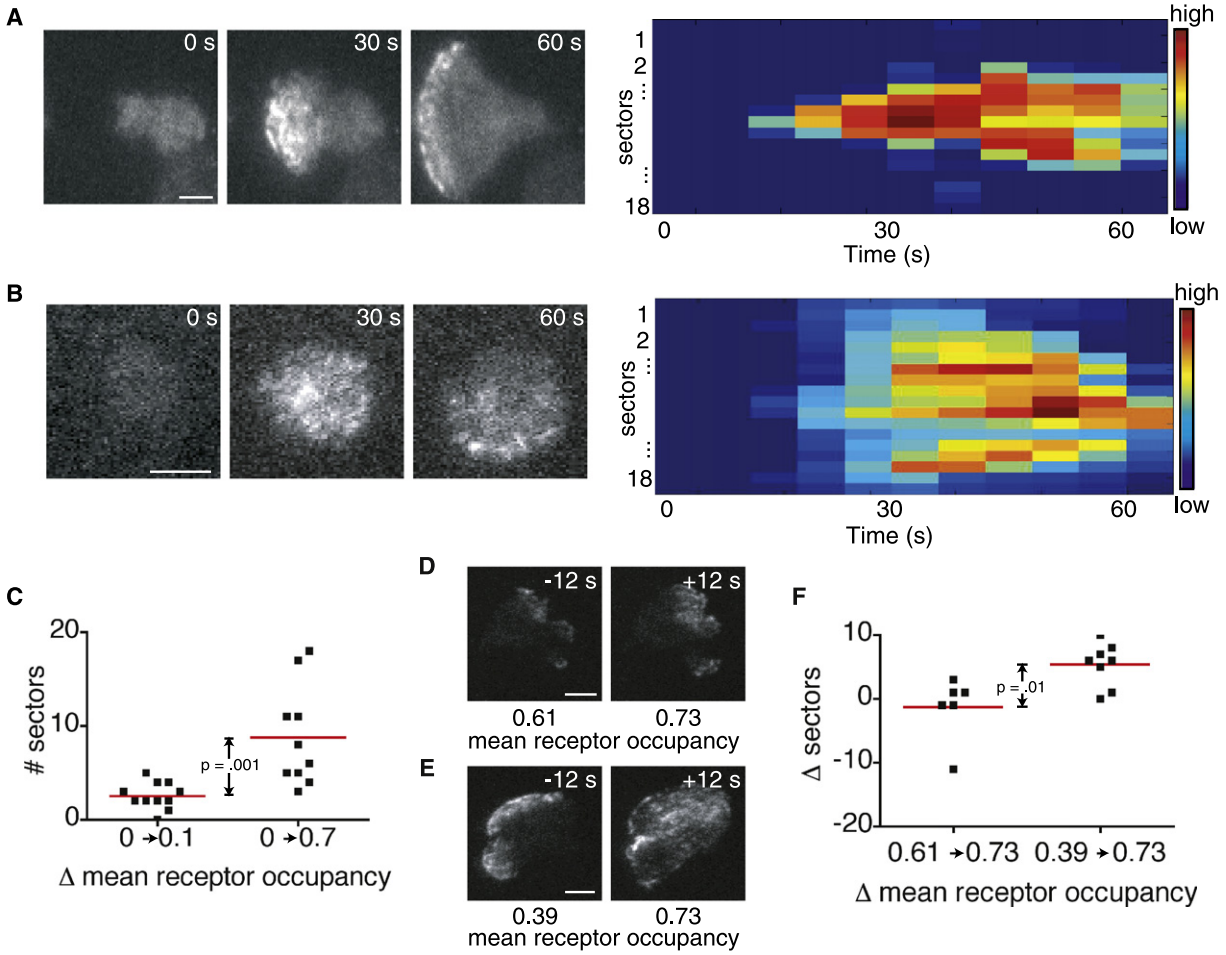

Figure 3. Directional Bias Limits Wave Generation in Response to Small Increases in Mean Receptor Occupancy

(A and B) Initially quiescent cells were subjected to spatially uniform increases in mean receptor occupancy from 0 to 0.1 (at t = 0 s), which produced focused waves (A) (Movie S6), or from 0 to 0.7 (at t = 0 s), which produced a spatially uniform distribution of Hem-1 waves that ultimately collapsed into a focused distribution (B) (Movie S7). Bars represent 5 μm.

(C) The dot plot shows a statistically significant difference (p = .001, Student's t test) between the mean widths (red lines) of the distributions.

(D and E) Representative time-lapse images of cells with prepolarized WAVE complex distributions responding to spatially uniform increases in mean receptor occupancy from (D) 0.61 to 0.73 (n = 6; Movie S8) or (E) 0.39 to 0.73 (n = 8; Movie S9).

(F) The dot plot shows a statistically significant difference (p = 0.01, Student's t test) between the changes in wave width for small versus large increases in mean receptor occupancy (note that mean receptor occupancies are statistically different even after removing the outlier for the 0.61 to 0.73 increase). These data suggest that intrinsic directional bias can maintain the asymmetric distribution of WAVE complex over a limited range of agonist concentrations in both quiescent and prepolarized cells.

restricts WAVE complex responses for intermediate increases in mean receptor occupancy (Figure 3D and Movie S8) in a manner similar to the role of an intrinsic bias during the establishment of polarity. However, larger steps of uniform agonist elicited uniform WAVE complex recruitment (Figures 3E and 3F and Movie S9), indicating that this bias can be overcome.

During chemotaxis, both an external bias from the agonist gradient and the cell's intrinsic biases could influence the establishment of WAVE complex asymmetries. In other cell types, such as *Dictyostelium*, only agonist gradients and not uniform chemoattractant produce signaling polarity [15]. Under these conditions, it is difficult to separate the effects of intrinsic biases from those of the external gradient. In contrast, neutrophils exhibit signaling polarity in uniform chemoattractant as well as gradients [17], enabling us to determine the role of internal directional bias independent of gradient sensing.

External gradients limit the spatial extent of WAVE complex recruitment for initially quiescent cells (Figure 2B). Here, external gradients set the final direction of WAVE complex polarity and overwhelm any internal signaling biases within the cell. This occurs for mean receptor-occupancy increases less than 0.63. In contrast, under a condition in which only internal signaling biases operate, a similar step size (an increase of 0.34) elicited uniform WAVE complex recruitment in polarized cells (Figure 3E). These data indicate that gradient sensing can overwhelm intrinsic biases and can constrain cell responses over a larger range of agonist increases than intrinsic biases.

Some cues such as PIP_3 can polarize in the absence of actin rearrangements [15, 17, 23, 24], but it is unclear whether WAVE complex asymmetry can also be uncoupled from downstream actin-dependent morphological rearrangements. We treated neutrophils with latrunculin to inhibit actin polymerization. Even in the absence of external agonist, latrunculin transiently increased the concentration of WAVE complex at the membrane (Figure 4A, 40 s). Under these conditions, the

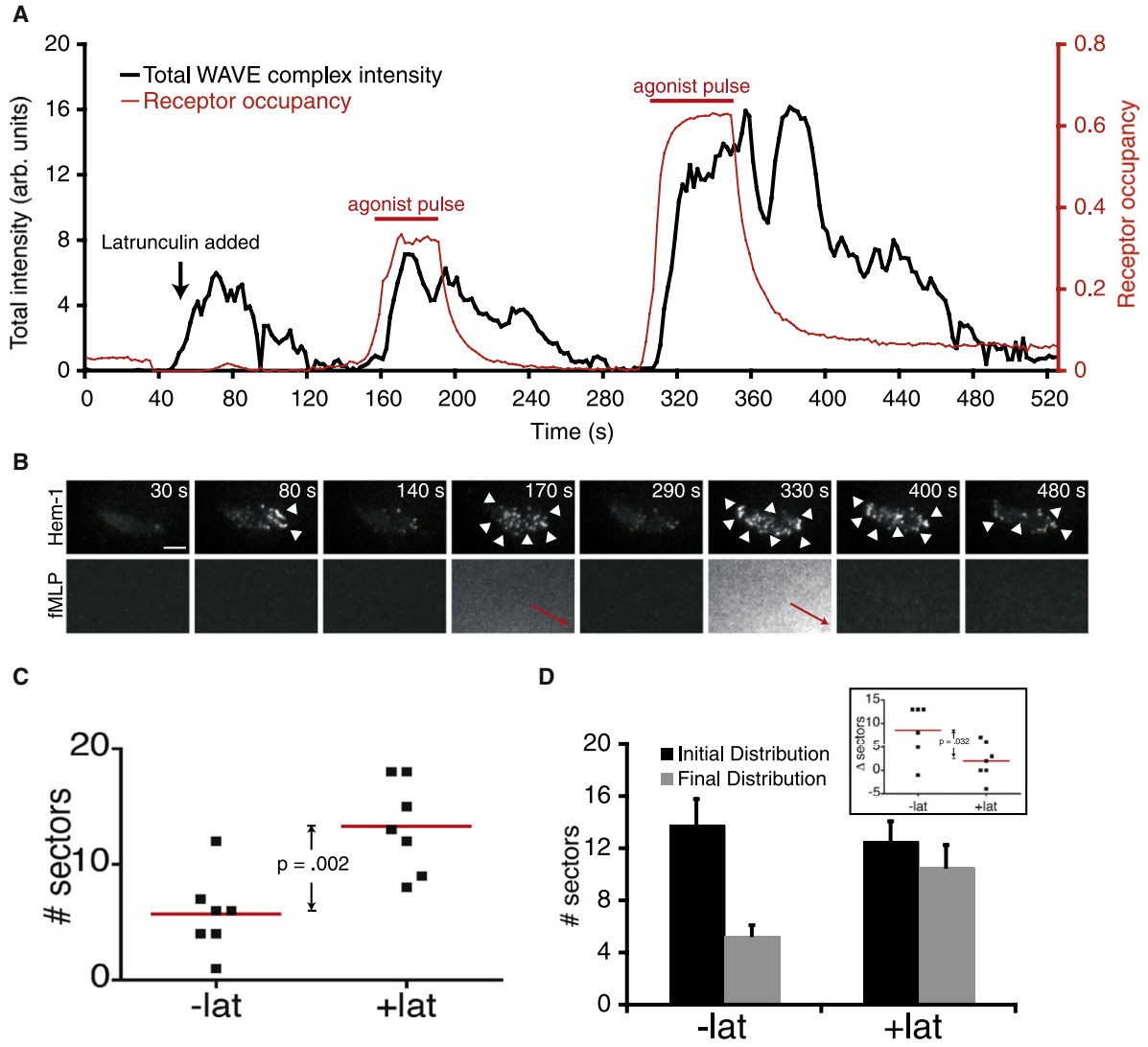

Figure 4. Actin Polymer Is Required for Establishment of Hem-1 Wave Asymmetry

(A) Transient formyl-methionyl-leucyl-phenylalanine (fMLP) pulses (red trace) induce transient Hem-1-YFP (black trace) accumulation at the membrane. An initially migrating cell was subjected to 20 μM latrunculin treatment for depolymerizing the actin cytoskeleton (40 s). This induced Hem-1-YFP recruitment even in the absence of external stimuli. Subsequent fMLP pulses from a micropipette (160 and 300 s) induced further recruitment. When the agonist was removed, Hem-1-YFP quickly disappeared from the membrane.

(B) Selected TIRF images (Movie S10) from the traces shown in (A). Red arrows indicate the direction of gradient pulses. Arrowheads indicate areas of significant Hem-1-YFP accumulation at the membrane. Note the broad distribution after each agonist pulse. The bar represents 5 μm.

(C) Dot plot of a 20 s average of wave response immediately after an agonist pulse for cells untreated (−lat) and treated with 20 μM latrunculin (+lat). There is a statistically significant difference between the mean widths (red lines) of the two populations ($p = .002$, Student's t test).

(D) Untreated cells that showed an initially broad wave distribution after an agonist pulse were compared to latrunculin-treated cells. The wave distribution in untreated cells converged into a focused distribution, whereas the wave distribution in latrunculin-treated cells did not converge. Error bars represent the SEM. The inset shows statistical significance between the differences in mean sectors (red lines) of the two populations ($p = .002$, Student's t test).

WAVE complex still responds to stimulation, although WAVE complex puncta are observed instead of propagating waves. Sudden addition of an agonist gradient increased WAVE complex recruitment (Figure 4A, 160 and 300 s), whereas removal of agonist caused WAVE complex release from the membrane (Figure 4A, 200 and 360 s). In latrunculin-treated cells exposed to gradients of chemoattractant, the localization of WAVE complex was relatively uniform (Figure 4B, 170 and 330 s, and Movie S10). Untreated cells typically produced focused WAVE complex recruitment in response to small increases in agonist gradients (Figure 2B). In contrast, latrunculin-treated cells that experienced a similar increase in receptor occupancy exhibited a significantly wider WAVE complex distribution (Figure 4C). Therefore, actin polymer, which is generated downstream of the WAVE complex, also appears to be required for the initial generation of WAVE complex asymmetry in neutrophils. Additionally, for control cells exposed to large increases in agonist gradients, the WAVE complex was initially relatively uniform but resolved into a more focused distribution over time. In contrast, this selection mechanism was not apparent over the timescale analyzed in latrunculin-treated cells (Figure 4D). Furthermore, previous studies implicate actin polymer as a factor that stabilizes signaling components at the membrane [25, 26], whereas

our data suggest that actin polymerization can also remove signaling proteins from the membrane.

We used biochemical fractionation to measure WAVE complex enrichment near the plasma membrane as a complement to our TIRF studies. A significant two-fold enrichment of the WAVE complex was observed in the plasma membrane fraction after stimulation and actin depolymerization, indicating that at least some of the TIRF-visible pool of the WAVE complex represents plasma membrane association (Figure S3).

Conclusions

Two models cover how cells reorient polarity during directional migration, and aspects of each apply to how cells initially establish polarity. One model showed that *Dicytostelium* respond by selectively retaining the pseudopod that experiences the highest agonist concentration, rather than biasing pseudopod generation [8]. In our system, the unit of selection is not a pseudopod, but rather smaller organizing units consisting of WAVE complex recruitment events. In contrast, the local generation model for chemotaxis proposes that the chemotactic behavior of the cell is the sum of local, independent protrusion events all over the surface of the pseudopod [7]. Once a cell is polarized, the probability of a protrusion event occurring in a particular location on the pseudopod depends on the relative local concentration of agonist. Extending this generation-based model to unpolarized cells can explain how a cell can initially bias WAVE complex asymmetry when receptor occupancy is low ($\sim$0.1), a phenomenon inexplicable by a selection-based model. However, the generation-based model fails to explain how cells could generate WAVE complex recruitment everywhere and selectively retain WAVE complex recruitment up-gradient, so each model succeeds where the other fails.

We propose a model in which local generation events are linked to cellular adaptation machinery. For small increases in agonist, a generation-based mechanism leads to immediately focused polarity. For larger increases in agonist, the generation machinery is saturated, resulting in a uniform WAVE complex distribution. In this case, global adaptation allows the cell to selectively retain WAVE complex recruitment to achieve WAVE asymmetry in a direction set by intrinsic biases or the external gradient. Our model enables the cell to balance rapid polarization (initial signal generation to the up-gradient side) with a more robust polarization (a slower gradual selection of uniform signal distribution, which can occur over a wider range of stimulation conditions). Importantly, the dominant mechanism of polarization depends on the amount of stimulation.

Intriguingly, actin polymerization is essential for WAVE complex polarization during chemotaxis. There are many examples of loss-of-function perturbations of chemotactic signaling that block intracellular signaling responses including PIP_3 generation, Ras and Rac activation, actin polymerization, and morphological changes in response to external chemoattractant [5, 26–32]. The WAVE complex is the first example of an intracellular signal that depends on actin polymer for its polarization, but not for its global responsiveness to stimulation.

Supplemental Data

Supplemental Data include Supplemental Experimental Procedures, three figures, and ten movies and can be found with this article online at http://www.current-biology.com/supplemental/S0960-9822(09)00537-5.

Acknowledgments

We thank John Sedat for image-denoising collaboration, the Nikon Imaging Center at UCSF for Matlab analysis software, Scott Foster for leukocyte preparation, and Henry Bourne, Oliver Hoeller, Steve Altschuler, Lani Wu, Max Krummel, Benjamin Rhau, Mark Von Zastrow, Alexander Watters, Sarah Wilson, Bryant Chhun, Delquin Gong, and Julie Wu for helpful comments on the manuscript. This work was supported by National Institutes of Health (NIH) R01 (GM084040), the UCSF/UCB Cell Propulsion Lab (an NIH Nanomedicine Development Center), a Searle Scholars Award, an American Heart Association National Scientist Development Grant, a National Defense Science and Engineering Graduate Fellowship to A.M., an American Heart Association Graduate Fellowship to A.H., and an Achievement Rewards for College Scientists Scholarship to S.D.

Received: September 16, 2008
Revised: December 19, 2008
Accepted: December 22, 2008
Published online: February 5, 2009

References

1. Machesky, L.M., and Insall, R.H. (1998). Scar1 and the related Wiskott-Aldrich syndrome protein, WASP, regulate the actin cytoskeleton through the Arp2/3 complex. Curr. Biol. *8*, 1347–1356.
2. Kunda, P., Craig, G., Dominguez, V., and Baum, B. (2003). Abi, Sra1, and Kette control the stability and localization of SCAR/WAVE to regulate the formation of actin-based protrusions. Curr. Biol. *13*, 1867–1875.
3. Steffen, A., Rottner, K., Ehinger, J., Innocenti, M., Scita, G., Wehland, J., and Stradal, T.E. (2004). Sra-1 and Nap1 link Rac to actin assembly driving lamellipodia formation. EMBO J. *23*, 749–759.
4. Stradal, T.E., and Scita, G. (2006). Protein complexes regulating Arp2/3-mediated actin assembly. Curr. Opin. Cell Biol. *18*, 4–10.
5. Weiner, O.D., Rentel, M.C., Ott, A., Brown, G.E., Jedrychowski, M., Yaffe, M.B., Gygi, S.P., Cantley, L.C., Bourne, H.R., and Kirschner, M.W. (2006). Hem-1 complexes are essential for Rac activation, actin polymerization, and myosin regulation during neutrophil chemotaxis. PLoS Biol. *4*, e38.
6. Weiner, O.D., Marganski, W.A., Wu, L.F., Altschuler, S.J., and Kirschner, M.W. (2007). An actin-based wave generator organizes cell motility. PLoS Biol. *5*, e221.
7. Arrieumerlou, C., and Meyer, T. (2005). A local coupling model and compass parameter for eukaryotic chemotaxis. Dev. Cell *8*, 215–227.
8. Andrew, N., and Insall, R.H. (2007). Chemotaxis in shallow gradients is mediated independently of PtdIns 3-kinase by biased choices between random protrusions. Nat. Cell Biol. *9*, 193–200.
9. Patel, F.B., Bernadskaya, Y.Y., Chen, E., Jobanputra, A., Pooladi, Z., Freeman, K.L., Gally, C., Mohler, W.A., and Soto, M.C. (2008). The WAVE/SCAR complex promotes polarized cell movements and actin enrichment in epithelia during C. elegans embryogenesis. Dev. Biol. *324*, 297–309.
10. Zallen, J.A., Cohen, Y., Hudson, A.M., Cooley, L., Wieschaus, E., and Schejter, E.D. (2002). SCAR is a primary regulator of Arp2/3-dependent morphological events in Drosophila. J. Cell Biol. *156*, 689–701.
11. Rogers, S.L., Wiedemann, U., Stuurman, N., and Vale, R.D. (2003). Molecular requirements for actin-based lamella formation in Drosophila S2 cells. J. Cell Biol. *162*, 1079–1088.
12. Rakeman, A.S., and Anderson, K.V. (2006). Axis specification and morphogenesis in the mouse embryo require Nap1, a regulator of WAVE-mediated actin branching. Development *133*, 3075–3083.
13. Hahne, P., Sechi, A., Benesch, S., and Small, J.V. (2001). Scar/WAVE is localised at the tips of protruding lamellipodia in living cells. FEBS Lett. *492*, 215–220.
14. Lai, F.P., Szczodrak, M., Block, J., Faix, J., Breitsprecher, D., Mannherz, H.G., Stradal, T.E., Dunn, G.A., Small, J.V., and Rottner, K. (2008). Arp2/3 complex interactions and actin network turnover in lamellipodia. EMBO J. *27*, 982–992.
15. Parent, C.A., Blacklock, B.J., Froehlich, W.M., Murphy, D.B., and Devreotes, P.N. (1998). G protein signaling events are activated at the leading edge of chemotactic cells. Cell *95*, 81–91.
16. Meili, R., Ellsworth, C., Lee, S., Reddy, T.B., Ma, H., and Firtel, R.A. (1999). Chemoattractant-mediated transient activation and membrane localization of Akt/PKB is required for efficient chemotaxis to cAMP in Dictyostelium. EMBO J. *18*, 2092–2105.

17. Servant, G., Weiner, O.D., Herzmark, P., Balla, T., Sedat, J.W., and Bourne, H.R. (2000). Polarization of chemoattractant receptor signaling during neutrophil chemotaxis. Science *287*, 1037–1040.
18. Zigmond, S.H., Levitsky, H.I., and Kreel, B.J. (1981). Cell polarity: An examination of its behavioral expression and its consequences for polymorphonuclear leukocyte chemotaxis. J. Cell Biol. *89*, 585–592.
19. Ferguson, G.J., Milne, L., Kulkarni, S., Sasaki, T., Walker, S., Andrews, S., Crabbe, T., Finan, P., Jones, G., Jackson, S., et al. (2007). PI(3)K-gamma has an important context-dependent role in neutrophil chemokinesis. Nat. Cell Biol. *9*, 86–91.
20. Hoeller, O., and Kay, R.R. (2007). Chemotaxis in the absence of PIP3 gradients. Curr. Biol. *17*, 813–817.
21. Xu, J., Van Keymeulen, A., Wakida, N.M., Carlton, P., Berns, M.W., and Bourne, H.R. (2007). Polarity reveals intrinsic cell chirality. Proc. Natl. Acad. Sci. USA *104*, 9296–9300.
22. Xu, J., Wang, F., Van Keymeulen, A., Herzmark, P., Straight, A., Kelly, K., Takuwa, Y., Sugimoto, N., Mitchison, T., and Bourne, H.R. (2003). Divergent signals and cytoskeletal assemblies regulate self-organizing polarity in neutrophils. Cell *114*, 201–214.
23. Janetopoulos, C., Ma, L., Devreotes, P.N., and Iglesias, P.A. (2004). Chemoattractant-induced phosphatidylinositol 3,4,5-trisphosphate accumulation is spatially amplified and adapts, independent of the actin cytoskeleton. Proc. Natl. Acad. Sci. USA *101*, 8951–8956.
24. Xu, X., Meier-Schellersheim, M., Yan, J., and Jin, T. (2007). Locally controlled inhibitory mechanisms are involved in eukaryotic GPCR-mediated chemosensing. J. Cell Biol. *178*, 141–153.
25. Devreotes, P., and Janetopoulos, C. (2003). Eukaryotic chemotaxis: Distinctions between directional sensing and polarization. J. Biol. Chem. *278*, 20445–20448.
26. Sasaki, A.T., Chun, C., Takeda, K., and Firtel, R.A. (2004). Localized Ras signaling at the leading edge regulates PI3K, cell polarity, and directional cell movement. J. Cell Biol. *167*, 505–518.
27. Shefcyk, J., Yassin, R., Volpi, M., Molski, T.F., Naccache, P.H., Munoz, J.J., Becker, E.L., Feinstein, M.B., and Sha'afi, R.I. (1985). Pertussis but not cholera toxin inhibits the stimulated increase in actin association with the cytoskeleton in rabbit neutrophils: Role of the "G proteins" in stimulus-response coupling. Biochem. Biophys. Res. Commun. *126*, 1174–1181.
28. Wu, L., Valkema, R., Van Haastert, P.J., and Devreotes, P.N. (1995). The G protein beta subunit is essential for multiple responses to chemoattractants in Dictyostelium. J. Cell Biol. *129*, 1667–1675.
29. Kumagai, A., Hadwiger, J.A., Pupillo, M., and Firtel, R.A. (1991). Molecular genetic analysis of two G alpha protein subunits in Dictyostelium. J. Biol. Chem. *266*, 1220–1228.
30. Sun, C.X., Downey, G.P., Zhu, F., Koh, A.L., Thang, H., and Glogauer, M. (2004). Rac1 is the small GTPase responsible for regulating the neutrophil chemotaxis compass. Blood *104*, 3758–3765.
31. Chen, L., Iijima, M., Tang, M., Landree, M.A., Huang, Y.E., Xiong, Y., Iglesias, P.A., and Devreotes, P.N. (2007). PLA2 and PI3K/PTEN pathways act in parallel to mediate chemotaxis. Dev. Cell *12*, 603–614.
32. Veltman, D.M., Keizer-Gunnik, I., and Van Haastert, P.J. (2008). Four key signaling pathways mediating chemotaxis in Dictyostelium discoideum. J. Cell Biol. *180*, 747–753.